10.1109/ULTSYM.2015.0380

Effects of Aberration in Crawling Wave Sonoelastography

Gabriela Torres[1], Kevin J. Parker[2], Benjamín Castañeda[1] and Roberto Lavarello[1]
[1]Laboratorio de Imágenes Médicas, Dpto. de Ingeniería, Pontificia Universidad Católica del Perú, Lima, Perú.
[2]Electrical and Computer Engineering Department, University of Rochester, New York, USA.

***Abstract*—Quantitative sonoelastography, through the formation of crawling waves, allows the estimation of elastic parameters in tissues using pulsed wave Doppler techniques. However, this technique's performance may be compromised by aberration effects during *in vivo* applications. In this study, an experimental evaluation of the effects of aberration when estimating shear wave speed from homogeneous phantoms was performed. The evaluations were performed using a commercial ultrasound scanner and gelatin-agar aberration layers of 33.26 ns, 62 ns and 116.73 ns RMS strength, and 2.00 mm, 3.40 mm and 6.70 mm of correlation length, respectively. The estimated speed values were obtained as a function of the vibration frequency for both the non-aberrated and aberrated cases. The estimated mean shear wave speed values in the presence of aberration showed only a 3% variation from those obtained in the non-aberrated cases. These experimental results suggest that crawling wave sonoelastography is not significantly affected by aberration effects in conditions typically observed in applications such as abdominal and breast imaging.**

Keywords—crawling wave sonoelastography; aberration; shear wave speed estimation.

I. Introduction

Sonoelastography is a noninvasive ultrasonic technique that allows the estimation of elastic properties using external mechanical vibrations [1]. Both qualitative and quantitative variants of this technique have been developed, typically using one and two vibration sources in the former and latter cases, respectively.

Crawling wave (CrW) sonoelastography is a quantitative method which allows the estimation of elastic parameters of tissue through the calculation of shear wave speed (SWS) using pulsed-wave Doppler techniques to monitor the shear waves produced by external mechanical vibrators. This technique has been applied in tissue mimicking phantoms, *ex vivo* and *in vivo* experiments, showing promising results [2, 3]. However, as the current CrW sonoelastography technique is based on the scanner assumption that the longitudinal ultrasonic wave propagation occurs at an invariant sound speed, its effectiveness for *in vivo* applications may diminished by aberration effects.

In ultrasound, aberration (i.e. the degradation of the wavefronts when propagating in inhomogeneous media) can significantly affect the quality of echographic imaging [4]. This degradation is a consequence of sound speed variations caused by different intervening tissues (such as fat and muscle when performing abdominal imaging) which degrade spatial resolution and contrast due to defocusing at the region of interest. As global obesity rates continue to rise [5], aberration becomes increasingly relevant for ultrasonic medical imaging.

Aberration has been shown to cause problems for quantitative elastographic techniques. Reports have shown that aberration produces relevant imaging alteration not only in acoustic radiation force (ARF) based techniques [6], but also in compression elasticity [7]. Even though these studies suggest that aberration may be a significant problem for elastographic tissue characterization, there has not yet been an evaluation of aberration effects on sonoelastographic examinations and specifically for the case of CrW sonoelastography.

This study has been conducted in order to provide a preliminary quantitative analysis of the impact of aberration in CrW sonoelastography. The effects on the generation of SWS maps were assessed through experimental CrW evaluations of a calibrated tissue-mimicking phantom using aberration layers of different aberration strengths.

II. Methods

A. Sonoelastography

The sonoelastography acquisition process starts with a sinusoidal vibration that is induced in the tissue by external mechanical vibrators. Radiofrequency data is acquired consecutively for a pre-defined number of emissions (i.e. ensemble length) at a given pulse repetition frequency (PRF). Sonoelastography data is then generated by applying Kasai's algorithm to estimate the variance σ^2 of the slow-time Doppler spectrum

$$\sigma^2 = \frac{2}{PRP}\left(1 - \frac{|R(PRP)|}{R(0)}\right), \quad [3]$$

where $R(x)$ is the autocorrelation of the in-phase and quadrature signals obtained for one ensemble. This process is repeated for several lines of data to form an image, where the estimated variance is proportional to the squared amplitude of the vibration in the tissue.

B. Shear wave speed generation

CrW sonoelastography is generated by vibrating two shakers located on opposite sides of the tissue with a small frequency difference (typically 0.4 Hz). With the variance of the slow-time Doppler spectrum obtained as described in section B, the spatial phase is processed for each coordinate in time through its Fourier transform, generating a phase map, as shown in Figure 1. Given the gradient for each coordinate of this phase map, the shear wave speed map can be calculated as,

$$c(x,y) = \frac{4\pi d(f_v + f_{offset})}{G(x,y)}, \quad [3]$$

where f_v represents the vibration frequency of one source, f_{offset} represents the difference between the vibration frequencies of the two sources, d represents the width of the analyzed zone, and G represents the spatial phase gradient.

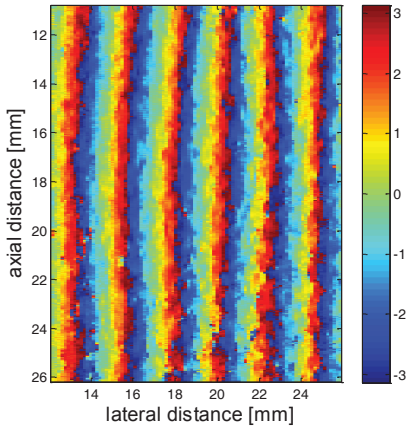

Fig. 1. Phase map (in radians) obtained from the variance of the slow-time Doppler spectrum.

C. CrW sonoelastography experiments

The experiments were designed to test the effects of aberration layers located in between the transducer and phantom when constructing CrW sonoelastography images using a range of vibration frequencies from 200 Hz to 300 Hz. An elasticity quality assurance phantom (model 049, CIRS Inc., Norfolk, VI, USA) was used to simulate the homogeneous tissue. For these experiments, an Ultrasonix SonixTouch scanner (Analogic Ultrasound, Peabody, MA, USA) equipped with a linear L14-5 transducer operated at 5 MHz was used.

The experimental setup is shown in Figure 2. A signal generator (model 4040B, B&K Precision Corp., Yorba Linda, CA, USA) and amplifier (model A-X500, TEAC, Tokyo, Japan) were connected to both shakers (model 4810, Brüel & Kjaer, Nærum, Denmark) in direct contact with the phantom. The aberration layer was located between the homogeneous phantom and the transducer, covered with gel on both sides.

D. Aberration layers

Aberration layers were constructed using the procedure in [8] with a combination of water, gelatin, agar and NaCl. The material was poured into custom-made 3D-printed molds in order to create layers based on designed aberration profiles with specific aberration strengths of 11 ns, 29 ns and 84 ns. As previous studies have reported aberration strength values ranging from 8 ns to 67 ns in human breast [9, 10] and from 12.9 ns to 29.7 ns in human abdominal wall [11, 12], the aberration layers were designed to cover the range from 10 ns to 90 ns in order to simulate conditions that are found in both applications.

The time delay profiles of the array were estimated using pre-beamformed data collected using a SonixTouch scanner (Analogic Ultrasound, Peabody, MA, USA) from the elasticity quality assurance phantom used in this study (model 049, CIRS Inc., Norfolk, VI, USA) with the aberration layers in between the phantom and the transducer. The ultrasound echoes were pre-steered and aberration profiles were estimated using the scaled covariance matrix (SCM) algorithm [13]. This procedure was repeated for all the aberration layers used in this study to estimate their actual properties (i.e. aberration strength and correlation length).

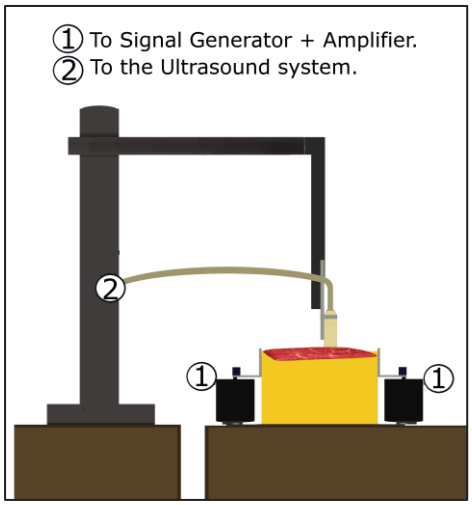

Fig. 2. Experimental setup of sonoelastography experiments. The shakers produce a periodic movement in the phantom that has an aberration layer on top. The transducer does not move and scans the vibrating scatterers.

III. Results

The properties of the different aberration layers are shown in Table 1. Layer 3 (L3) is producing the most RMS arrival time or strongest aberration and Layer 1 (L1) the weakest. This table shows the comparison of the time delay profiles obtained with the SCM algorithm for the three layers on top of the phantom. All three aberrator layers fitted the proposed ranges according to the design methodology explained in II D.

TABLE I. Experimental Properties of the Aberration Layers

Layer	*Aberration strength (ns)*	*Correlation length (mm)*
L1	18.72	4.79
L2	26.49	4.28
L3	82.50	4.57

Figures 3 and 4 show the SWS values obtained using vibration frequencies of 200 Hz and 300 Hz, respectively. The SWS maps obtained do not exhibit an increase of artifacts due to aberration. In fact, in Figure 5, the map obtained with the aberration layer L3 exhibited less pronounced artifacts compared to the map obtained without the aberration layer.

The estimated SWS values as a function of the vibration frequency are shown in Figure 5 for the non-aberrated and aberrated cases. The estimated mean SWS values in the presence of the L3 aberrator were nearly identical to the ones obtained in the non-aberrated case. The standard deviation did not increase by more than 10% for all the cases. Further, the mean estimated SWS value was in good agreement with the SWS value reported by the manufacturer (i.e., 2.95 ms^{-1}) for all cases.

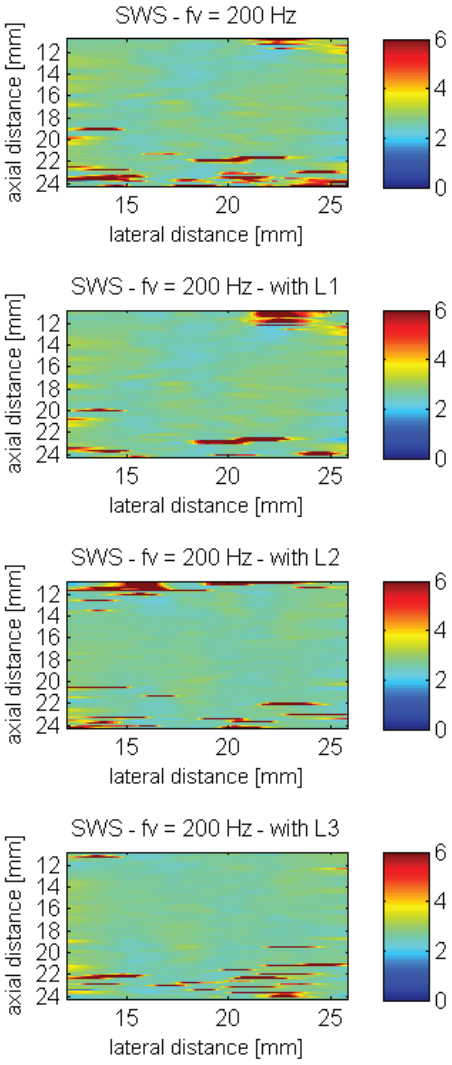

Fig. 3. SWS maps (in ms^{-1}) using a vibration frequency of 200 Hz for the homogeneous phantom. From top to bottom: without an aberrator, with aberrator L1, L2 and L3 respectively.

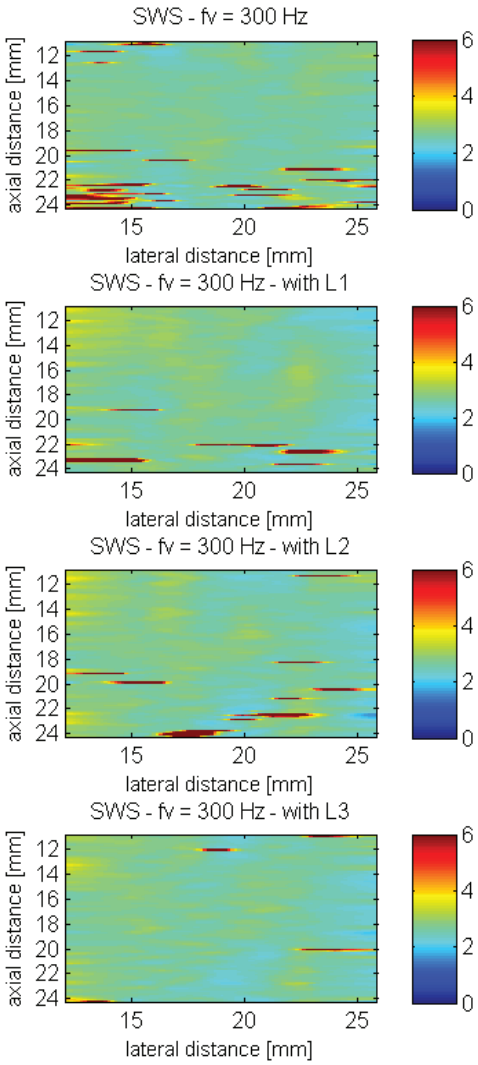

Fig. 4. SWS maps (in ms^{-1}) using a vibration frequency of 300 Hz for the homogeneous phantom. From top to bottom: without an aberrator, with aberrator L1, L2 and L3 respectively.

IV. Discussion

The estimated SWS values as a function of the vibration frequency presented in Figure 5 suggest that the aberration effects in CrW sonoelastography when imaging homogeneous media appear to be minor.

The estimated mean SWS values in the presence of aberration were nearly identical to the SWS value presented by the manufacturer. The most accurate estimates were obtained with the L1 and L3 aberrators, which resulted in a variation of less than 0.5% from the expected SWS value. In the case of the L2 aberrator and no aberrator, the bias was less than 3%, which indicates that the results presented high accuracy for all tested experimental conditions.

In terms of precision, the estimated SWS maps for all the cases presented a standard deviation value of less than 15%. The SWS images of the phantom without an aberrator and with the L1, L2, and L3 aberrators presented variations of 12.96%, 14.61%, 14.97%, and 14.72% respectively. Therefore, the variability increment between the aberrated and non-aberrated cases was not significant. Moreover, for the range of aberration strengths and vibration frequencies used in this study, no correlation between the SWS standard deviation and the aberration strength was found.

Comparing the data obtained in this study with previous aberration reports for other Doppler-based techniques [16], the results are expected. Additionally, this behavior stands CrW from other ARF-based techniques that present effects on the image formation [6, 17]. The presented experimental results suggest that CrW sonoelastography may not be significantly affected by aberration effects.

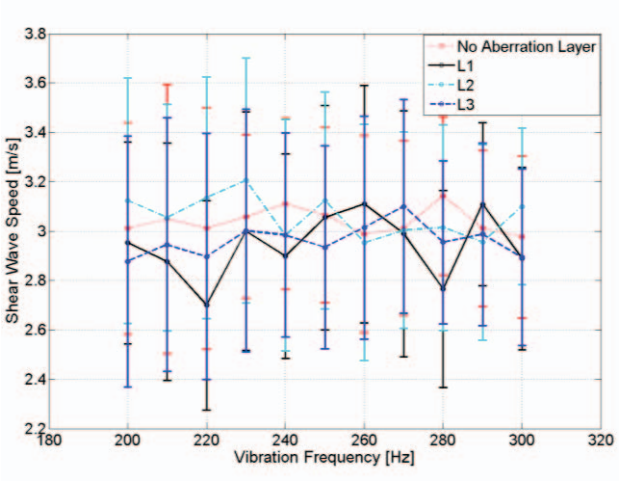

Fig. 5. Comparison of estimated SWS mean and standard deviation values for different vibration frequencies using the homogeneous phantom with no aberration layer (red dotted line), with L1 layer (black solid line), with L2 layer (cyan dashed and dotted line), and with L3 layer (blue dashed line) on top.

However, additional studies are necessary in order to address further effects of aberration in more complex conditions when using CrW sonoelastography. SWS maps of phantoms with inclusions should also be affected by the loss in spatial resolution under aberrating conditions, an effect that may not be significant when imaging homogeneous media. Further, recent works have addressed the application of phase aberration correction methods in quantitative ultrasound techniques to compensate for aberration effects on transmission and reception beams [18]. Therefore, the usefulness of phase aberration correction in combination with CrW sonoelastography should also be explored.

V. Conclusion

The experimental results suggest that CrW sonoelastography is not significantly affected by aberration effects. For aberration strengths of 18.72 ns, 26.49 ns and 82.50 ns, the variance of the SWS obtained in homogeneous phantoms did not increased more than a 3%.

Acknowledgment

The authors would like to thank Gustavo Chau for his technical assistance with this study. This research was supported by grant 012-2014-FONDECYT-C1 from the Peruvian Government and PUCP grant DGI-2013-0131.

References

[1] R. M. Lerner, K. J. Parker, J. Holen, R. Gramiak, R. C. Waag, "Sonoelasticity: Medical elasticity images derived from ultrasound signals in mechanically vibrated targets," in *Proceedings of the International Symposium of Acoustical Imaging*, no. 16, pp. 317-327, 1988.

[2] B. Castaneda, L. An, S. Wu, L.L. Baxter, J.L. Yao, J. V. Joseph, K. Hoyt, J. Strang, D. J Rubens, Kevin J Parker, "Prostate cancer detection using crawling wave sonoelastography," in *Proceedings of the SPIE Medical Imaging*, no. 7265, pp. 1301-1310, 2009.

[3] A. Partin, Z. Hah, C. T. Barry, D. J. Rubens, K. J. Parker, "Elasticity estimates from images of crawling waves generated by miniature surface sources," *Ultrasound in Medicine & Biology*, no. 40, pp. 685-694, 2014.

[4] O'Donnell, S.W. Flax, "Phase aberration measurements in medical ultrasound: Human studies," *Ultrasonic Imaging*, vol. 10, no. 1, pp. 1 – 11, 1988.

[5] World Health Organization, "Obesity and Overweight," *WHO Media Centre*, Fact Sheet N°311, 2015.

[6] C. Amador, S. Aristizabal, J. F. Greenleaf, M. W. Urban, "Effects of phase aberration on acoustic radiation force-based shear wave generation," in *Proceedings of the IEEE International Ultrasonic Symposium*, pp. 348-351, 2013.

[7] A. T. Fernandez, H. Xie, "Phase Aberration Effects in Static Compression Elasticity Imaging," in *Proceedings of the IEEE International Ultrasonics Symposium*, pp. 1051-601, 2006.

[8] E. L. Madsen, M. A. Hobson, H. Shi, T. Varghese, G. R. Frank, "Tissue-mimicking agar/gelatin materials for use in heterogeneous elastography phantoms," *Phys. Med. Biol*., vol. 50, pp. 5597–5618, 2005.

[9] S. A. Goss, R. L. Johnston, and F. Dunn, "Compilation of empirical ultrasonic properties of mammalian tissues," *J. Acoust. Soc. Amer*., vol. 64, no. 2, pp. 423–457, 1978.

[10] S. A. Goss, R. L. Johnston, and F. Dunn, "Compilation of empirical ultrasonic properties of mammalian tissues, II," *J. Acoust. Soc. Amer*., vol. 68, no. 1, pp. 93–108, 1980.

[11] L. M. Hinkelman, T. L. Szabo, and R. C. Waag, "Measurements of ultrasonic pulse distortion produced by human chest wall," *J. Acoust. Soc. Amer*., vol. 101, no. 4, pp. 2365–2373, 1997.

[12] L. M. Hinkelman, D.-L. Liu, L. A. Metlay, and R. C. Waag, "Measurements of ultrasonic pulse arrival time and energy level variations produced by propagation through abdominal wall," *J. Acoust. Soc. Amer*., vol. 95, no. 1, pp. 530–541, 1994.

[13] S. D. Silverstein, D. P. Ceperley, "Autofocusing in medical ultrasound: the scaled covariance matrix algorithm," *IEEE Transactions On Ultrasonics, Ferroelectrics, and Frequency Control*, vol. 50, pp. 795-804, 2003.

[14] M. E. Anderson, M.S. McKeag, G.E. Trahey, "The impact of sound speed errors on medical ultrasound imaging," *J. Acoust. Soc. Amer.*, vol. 107, no. 6, pp. 3540-3548, 2000.

[15] J. J. Dahl, G. E. Trahey, G. F. Pinton, "The effects of image degradation on ultrasound-guided HIFU," in *Proceedings of the IEEE International Ultrasonics Symposium*, pp. 809-812, 2010.

[16] H. Xie, V. Shamdasani, A. T. Fernandez, R. Peterson, M. Lachman, Y. Shi, J. Robert, M. Urban, S. Chen, J. Greenleaf, "Shear wave Dispersion Ultrasound Vibrometry (SDUV) on an ultrasound system: In vivo measurement of liver viscoelasticity in healthy animals," in *Proceedings of the IEEE International Ultrasonics Symposium*, pp. 912-915, 2010.

[17] M. L. Palmeri, M. H. Wang, N. C. Rouze, M. F. Abdelmalek, C. D Guy, B. Moser, A. M. Diehl, K. R. Nightingale, "Noninvasive Evaluation of Hepatic Fibrosis using Acoustic Radiation Force-Based Shear Stiffness in Patients with Nonalcoholic Fatty Liver Disease," *Journal of Hepatology*, vol. 55, no. 3 , pp. 666–672, 2011.

[18] E. Gonzalez, N. Seth, B. Castañeda, J. Dahl, R. Lavarello, "Accuracy of backscatter coefficient estimation in aberrating media using different phase aberration correction strategies - A simulation study," in *Proceedings of the IEEE International Ultrasonics Symposium*, pp. 2438 – 2441, 2014.